

Memory-efficient compression of \mathcal{DH}^2 -matrices for high-frequency Helmholtz problems

Steffen Börm and Janne Henningsen

October 4, 2023

Directional interpolation is a fast and efficient compression technique for high-frequency Helmholtz boundary integral equations, but requires a very large amount of storage in its original form. Algebraic recompression can significantly reduce the storage requirements and speed up the solution process accordingly. During the recompression process, weight matrices are required to correctly measure the influence of different basis vectors on the final result, and for highly accurate approximations, these weight matrices require more storage than the final compressed matrix.

We present a compression method for the weight matrices and demonstrate that it introduces only a controllable error to the overall approximation. Numerical experiments show that the new method leads to a significant reduction in storage requirements.

1 Introduction

We consider boundary element discretizations of the Helmholtz equation

$$-\Delta u - \kappa^2 u = 0$$

with the *wave number* $\kappa \in \mathbb{R}$ on a domain $\Omega \subseteq \mathbb{R}^3$. Using the fundamental solution

$$g(x, y) = \frac{\exp(i\kappa\|x - y\|)}{4\pi\|x - y\|} \quad \text{for all } x, y \in \mathbb{R}^3, x \neq y, \quad (1)$$

the boundary integral formulation leads to an equation of the form

$$\int_{\partial\Omega} g(x, y) \frac{\partial u}{\partial n}(y) dy = \frac{1}{2}u(x) + \int_{\partial\Omega} \frac{\partial g}{\partial n_y}(x, y) u(y) dy \quad \text{for all } x \in \partial\Omega \quad (2)$$

that allows us to compute the Neumann boundary values $\frac{\partial u}{\partial n}$ on $\partial\Omega$ from the Dirichlet boundary values. Once we know both, the solution u can be evaluated anywhere in the domain Ω .

In order to solve the integral equation (2), we employ a Galerkin discretization: the unknown Neumann values are approximated by a boundary element basis $(\varphi_i)_{i \in \mathcal{I}}$ and the Dirichlet values by another, possibly different, basis $(\psi_j)_{j \in \mathcal{J}}$. The discretization replaces the integral operators by matrices $G \in \mathbb{C}^{\mathcal{I} \times \mathcal{I}}$ and $K \in \mathbb{C}^{\mathcal{I} \times \mathcal{J}}$ given by

$$\begin{aligned} g_{ij} &:= \int_{\partial\Omega} \varphi_i(x) \int_{\partial\Omega} g(x, y) \varphi_j(y) dy dx && \text{for all } i, j \in \mathcal{I}, \\ k_{ij} &:= \int_{\partial\Omega} \varphi_i(x) \int_{\partial\Omega} \frac{\partial g}{\partial n_y}(x, y) \psi_j(y) dy dx && \text{for all } i \in \mathcal{I}, j \in \mathcal{J}. \end{aligned}$$

Both matrices are densely populated in general, and having to store them explicitly would severely limit the resolution and therefore the accuracy of the approximation.

Local low-rank approximations offer an attractive solution: if the kernel function can be approximated by a tensor product, the corresponding part of the matrix can be approximated by a low-rank matrix, and keeping this matrix in factorized form will significantly reduce the storage requirements.

Directional interpolation [6, 8, 5, 3] offers a particularly convenient approach: the kernel function is split into a plane wave and a smooth remainder, and interpolation of the remainder yields a tensor-product approximation of the kernel function. Advantages of this approach include ease of implementation and very robust convergence properties. A major disadvantage is the large amount of storage required by this approximation.

Fortunately, this disadvantage can be overcome by combining the analytical approximation with an algebraic recompression [2, 4] to significantly reduce the storage requirements and improve the speed of matrix-vector multiplications at the expense of some additional work. In order to guarantee the quality of the recompression, the algorithm relies on weight matrices that describe how “important” different basis vectors are for the final approximation.

If we are considering problems with high wave numbers and high resolutions, these weight matrices may require far more storage than the final result of the compression, i.e., we may run out of storage even if the final result would fit a given computer system.

To solve this problem, we present an algorithm for replacing the exact weight matrices by compressed weight matrices. The key challenge is to ensure that the additional errors introduced by this procedure can be controlled and do not significantly reduce the accuracy of the final result of the computation.

The following Section 2 introduces the structure of \mathcal{DH}^2 -matrices used to represent operators for high-frequency Helmholtz boundary integral equations. Section 3 shows how algebraic compression can be applied to significantly reduce the storage requirements of \mathcal{DH}^2 -matrices. Section 4 is focused on deriving error estimates for the compression. In Section 5, we introduce an algorithm for approximating the weight matrices while preserving the necessary accuracy. Section 6 contains numerical results indicating that the new method preserves the convergence rates of the underlying Galerkin discretization.

2 \mathcal{DH}^2 -matrices

Integral operators with smooth kernel functions can be handled efficiently by applying interpolation to the kernel function, since this gives rise to a low-rank approximation.

The kernel function of the high-frequency Helmholtz equation is oscillatory and therefore not well-suited for interpolation. The idea of directional interpolation [6, 8, 5] is to split the kernel function into an oscillatory part that can be approximated by a plane wave and a smooth part that can be approximated by interpolation.

2.1 Directional interpolation

To illustrate this approach, we approximate the oscillatory part $\exp(\iota\kappa\|x-y\|)$ for $x \in \tau$, $y \in \sigma$, where $\tau, \sigma \subseteq \mathbb{R}^3$ are star-shaped subsets with respect to centers $x_\tau \in \tau$ and $y_\sigma \in \sigma$. A Taylor expansion of $z := x - y$ around $z_0 := x_\tau - y_\sigma$ yields

$$\begin{aligned} \kappa\|z\| &= \kappa\|z_0\| + \kappa\left\langle \frac{z_0}{\|z_0\|}, z - z_0 \right\rangle \\ &+ \kappa \int_0^1 (1-t) \sin^2 \angle(z - z_0, z_0 + t(z - z_0)) \frac{\|z - z_0\|^2}{\|z_0 + t(z - z_0)\|} dt. \end{aligned}$$

Inserted into the exponential function, the first two terms on the right-hand side correspond to a plane wave. In order to ensure that this plane wave is a reasonably good approximation of the spherical wave appearing in the kernel function, we have to bound the integral term. Using the diameter and distance given by

$$\begin{aligned} \text{diam}(\tau) &:= \max\{\|x_1 - x_2\| : x_1, x_2 \in \tau\}, \\ \text{dist}(\tau, \sigma) &:= \min\{\|x - y\| : x \in \tau, y \in \sigma\}, \end{aligned}$$

the third term is bounded if

$$\kappa \max\{\text{diam}(\tau)^2, \text{diam}(\sigma)^2\} \leq \eta_3 \text{dist}(\tau, \sigma) \quad (3a)$$

holds with a suitable parameter $\eta_3 \in \mathbb{R}_{>0}$. In terms of our kernel function, this means that we can approximate the spherical wave $\exp(\iota\kappa\|x-y\|)$ by the plane wave travelling in direction z_0 .

Since z_0 depends on x_τ and y_σ , we would have to use different directions for every pair (τ, σ) of subdomains, and this would make the approximation too expensive. To keep the number of directions under control, we restrict ourselves to a fixed set \mathcal{D} of unit vectors and approximate $z_0/\|z_0\|$ by an element $c \in \mathcal{D}$. If we can ensure

$$\kappa \left\| \frac{x_\tau - y_\sigma}{\|x_\tau - y_\sigma\|} - c \right\| \max\{\text{diam}(\tau), \text{diam}(\sigma)\} \leq \eta_2 \quad (3b)$$

with a parameter $\eta_2 \in \mathbb{R}_{>0}$, the spherical wave divided by the plane wave

$$\frac{\exp(\iota\kappa\|x-y\|)}{\exp(\iota\kappa\langle c, x-y \rangle)} = \exp(\iota\kappa(\|x-y\| - \langle c, x-y \rangle))$$

will still be sufficiently smooth, and the modified kernel function

$$g_c(x, y) := \frac{\exp(\iota\kappa(\|x - y\| - \langle c, x - y \rangle))}{4\pi\|x - y\|} \quad \text{for all } x \in \tau, y \in \sigma$$

will no longer be oscillatory. In order to interpolate this function, we also have to keep its denominator under control. This can be accomplished by requiring

$$\max\{\text{diam}(\tau), \text{diam}(\sigma)\} \leq \eta_1 \text{dist}(\tau, \sigma). \quad (3c)$$

If the three *admissibility conditions* (3a), (3b), and (3c) hold, standard tensor interpolation of g_c converges at a robust rate [5, 3].

We choose interpolation points $(\xi_{\tau,\nu})_{\nu=1}^k$ with corresponding Lagrange polynomials $(\ell_{\tau,\nu})_{\nu=1}^k$ in the subdomain τ and interpolation points $(\xi_{\sigma,\mu})_{\mu=1}^k$ with corresponding Lagrange polynomials $(\ell_{\sigma,\mu})_{\mu=1}^k$ in the subdomain σ and approximate g_c by the interpolating polynomial

$$\tilde{g}_{\tau\sigma c}(x, y) := \sum_{\nu=1}^k \sum_{\mu=1}^k g_c(\xi_{\tau,\nu}, \xi_{\sigma,\mu}) \ell_{\tau,\nu}(x) \overline{\ell_{\sigma,\mu}(y)}.$$

In order to obtain an approximation of the original kernel function g , we have to multiply g_c by the plane wave $\exp(\iota\kappa\langle c, x - y \rangle)$ and get

$$\tilde{g}_{\tau\sigma}(x, y) = \sum_{\nu=1}^k \sum_{\mu=1}^k g_c(\xi_{\tau,\nu}, \xi_{\sigma,\mu}) \ell_{\tau,\nu}(x) \overline{\ell_{\sigma,\mu}(y)}$$

with the modified Lagrange functions

$$\ell_{\tau,\nu}(x) = \exp(\iota\kappa\langle c, x \rangle) \ell_{\tau,\nu}(x), \quad \ell_{\sigma,\mu}(y) = \exp(\iota\kappa\langle c, y \rangle) \ell_{\sigma,\mu}(y),$$

where we exploit

$$\overline{\ell_{\sigma,\mu}(y)} = \overline{\exp(\iota\kappa\langle c, y \rangle)} \ell_{\sigma,\mu}(y) = \exp(-\iota\kappa\langle c, y \rangle) \ell_{\sigma,\mu}(y) \quad \text{for all } y \in \mathbb{R}^3, \mu \in [1 : k].$$

2.2 \mathcal{DH}^2 -matrices

To obtain an approximation of the entire matrix G , we have to partition its index set $\mathcal{I} \times \mathcal{I}$ into subsets where our approximation can be used.

Definition 1 (Cluster tree) *Let \mathcal{T} be a finite tree, and let each of its nodes $t \in \mathcal{T}$ be associated with a subset $\hat{t} \subseteq \mathcal{I}$.*

\mathcal{T} is called a cluster tree for the index set \mathcal{I} if

- the root $r = \text{root}(\mathcal{T})$ is associated with $\hat{r} = \mathcal{I}$,
- for all $t \in \mathcal{T}$ with children, we have

$$\hat{t} = \bigcup_{t' \in \text{chil}(t)} \hat{t}'.$$

- for all $t \in \mathcal{T}$, $t_1, t_2 \in \text{chil}(t)$, we have

$$t_1 \neq t_2 \Rightarrow \hat{t}_1 \cap \hat{t}_2 = \emptyset.$$

A cluster tree for \mathcal{I} is usually denoted by $\mathcal{T}_{\mathcal{I}}$. Its leaves are denoted by $\mathcal{L}_{\mathcal{I}} := \{t \in \mathcal{T}_{\mathcal{I}} : \text{chil}(t) = \emptyset\}$.

A cluster tree provides us with a hierarchy of subsets of the index set \mathcal{I} , and its leaves define a disjoint partition of \mathcal{I} . In order to define approximations for the matrix G , we require a similar tree structure with subsets of $\mathcal{I} \times \mathcal{I}$.

Definition 2 (Block tree) Let \mathcal{T} be a finite tree. It is called a block tree for the cluster tree $\mathcal{T}_{\mathcal{I}}$ if

- for all $b \in \mathcal{T}$ there are $t, s \in \mathcal{T}_{\mathcal{I}}$ with $b = (t, s)$,
- the root $r = \text{root}(\mathcal{T})$ is given by $r = (\text{root}(\mathcal{T}_{\mathcal{I}}), \text{root}(\mathcal{T}_{\mathcal{I}}))$,
- for all $b = (t, s) \in \mathcal{T}$ with $\text{chil}(b) \neq \emptyset$ we have

$$\text{chil}(b) = \text{chil}(t) \times \text{chil}(s).$$

A block tree for $\mathcal{T}_{\mathcal{I}}$ is usually denoted by $\mathcal{T}_{\mathcal{I} \times \mathcal{I}}$. Its leaves are denoted by $\mathcal{L}_{\mathcal{I} \times \mathcal{I}} := \{b \in \mathcal{T}_{\mathcal{I} \times \mathcal{I}} : \text{chil}(b) = \emptyset\}$.

The definition implies that a block tree $\mathcal{T}_{\mathcal{I} \times \mathcal{I}}$ for $\mathcal{T}_{\mathcal{I}}$ is indeed a cluster tree for the index set $\mathcal{I} \times \mathcal{I}$, and therefore the leaves $\mathcal{L}_{\mathcal{I} \times \mathcal{I}}$ of a block tree describe a disjoint partition of $\mathcal{I} \times \mathcal{I}$, i.e., a decomposition of G into submatrices $G|_{\hat{t} \times \hat{s}}$ for all $b = (t, s) \in \mathcal{L}_{\mathcal{I} \times \mathcal{I}}$.

We cannot expect to be able to approximate the submatrices intersecting the diagonal due to the kernel function's singularity, but we can use the conditions (3) to choose those leaves of $\mathcal{T}_{\mathcal{I} \times \mathcal{I}}$ that can be approximated.

In order to be able to apply (3), we need to take the supports of the basis functions into account. Since we will be using tensor interpolation, we choose for every cluster $t \in \mathcal{T}_{\mathcal{I}}$ an axis-parallel *bounding box* $\tau \subseteq \mathbb{R}^3$ such that

$$\text{supp } \varphi_i \subseteq \tau \quad \text{for all } i \in \hat{t}.$$

For every cluster $s \in \mathcal{T}_{\mathcal{I}}$, we denote the corresponding bounding box by σ . If we have a block $(t, s) \in \mathcal{L}_{\mathcal{I} \times \mathcal{I}}$ with bounding boxes τ and σ satisfying the *admissibility conditions* (3), we can expect the approximation

$$\tilde{g}_{\tau\sigma}(x, y) = \sum_{\nu=1}^k \sum_{\mu=1}^k g_c(\xi_{\tau,\nu}, \xi_{\sigma,\mu}) \ell_{\tau c, \nu}(x) \overline{\ell_{\sigma c, \mu}(y)} \quad \text{for all } x \in \tau, y \in \sigma$$

for a suitably chosen direction c to converge rapidly and therefore

$$\begin{aligned}
g_{ij} &\approx \int_{\partial\Omega} \varphi_i(x) \int_{\partial\Omega} \tilde{g}_{\tau\sigma}(x, y) \varphi_j(y) dy dx \\
&= \sum_{\nu=1}^k \sum_{\mu=1}^k \underbrace{\int_{\partial\Omega} \ell_{\tau c, \nu}(x) \varphi_i(x) dx}_{=:v_{tc, i\nu}} \underbrace{g_c(\xi_{\tau, \nu}, \xi_{\sigma, \mu})}_{=:s_{ts, \nu\mu}} \underbrace{\int_{\partial\Omega} \overline{\ell_{\sigma c, \mu}(y) \varphi_j(y)} dy}_{=:v_{sc, j\mu}} \\
&= (V_{tc} S_{ts} V_{sc}^*)_{ij} \quad \text{for all } i \in \hat{t}, j \in \hat{s}.
\end{aligned} \tag{4}$$

This means that the submatrices corresponding to the leaves

$$\mathcal{L}_{\mathcal{I} \times \mathcal{I}}^+ := \{(t, s) \in \mathcal{L}_{\mathcal{I} \times \mathcal{I}} : \tau \text{ and } \sigma \text{ satisfy (3)}\}$$

can be approximated by low-rank matrices in factorized form.

We can satisfy the admissibility condition (3b) only if large clusters are accompanied by a large number of directions to choose from.

Definition 3 (Directions) *Let $\mathcal{T}_{\mathcal{I}}$ be a cluster tree. For every cluster $t \in \mathcal{T}_{\mathcal{I}}$ we let either $\mathcal{D}_t = \{0\}$ or choose a subset $\mathcal{D}_t \subseteq \mathbb{R}^3$ such that*

$$\|c\| = 1 \quad \text{for every } c \in \mathcal{D}_t.$$

The family $(\mathcal{D}_t)_{t \in \mathcal{T}_{\mathcal{I}}}$ is called a family of directions for the cluster tree $\mathcal{T}_{\mathcal{I}}$.

Allowing $\mathcal{D}_t = \{0\}$ makes algorithms more efficient for small clusters where (3b) can be fulfilled by choosing $c = 0$. In this case, the function $\ell_{\tau c, \nu}$ becomes simply the Lagrange polynomial $\ell_{\tau, \nu}$, and the modified kernel function g_c becomes just the standard kernel function g .

Storing the matrices $(V_{tc})_{t \in \mathcal{T}_{\mathcal{I}}, c \in \mathcal{D}_t}$ for all clusters and all directions would generally require $\mathcal{O}(n^2)$ coefficients, where $n = \#\mathcal{I}$ denotes the number of basis functions, and this would not be an improvement over simply storing the matrix explicitly. This problem can be overcome by taking advantage of the fact that we can approximate V_{tc} in terms of the matrices $V_{t'c'}$ corresponding to its children: if we use the same polynomial order for all clusters, we have

$$\ell_{\tau, \nu} = \sum_{\nu'=1}^k \ell_{\tau, \nu}(\xi_{\tau', \nu'}) \ell_{\tau', \nu'} \quad \text{for all } \nu \in [1 : k]$$

by the identity theorem, and interpolating a slightly modified function instead yields

$$\begin{aligned}
\ell_{\tau c, \nu}(x) &= \exp(\iota\kappa\langle c, x \rangle) \ell_{\tau, \nu}(x) \\
&= \exp(\iota\kappa\langle c', x \rangle) \exp(\iota\kappa\langle c - c', x \rangle) \ell_{\tau, \nu}(x) \\
&\approx \exp(\iota\kappa\langle c', x \rangle) \sum_{\nu'=1}^k \underbrace{\exp(\iota\kappa\langle c - c', \xi_{\tau', \nu'} \rangle)}_{=:e_{\tau' c, \nu' \nu}} \ell_{\tau, \nu}(\xi_{\tau', \nu'}) \ell_{\tau', \nu'}(x) \\
&= \sum_{\nu'=1}^k e_{\tau' c, \nu' \nu} \ell_{\tau' c', \nu'}(x),
\end{aligned}$$

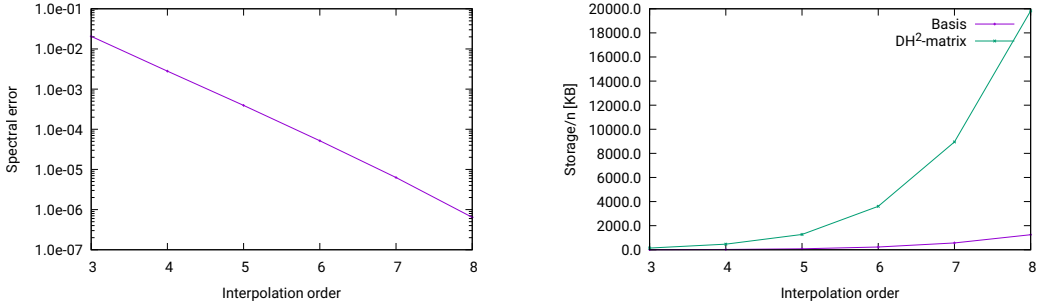


Figure 1: Left: Convergence of directional interpolation with increasing order. Right: Storage requirements with increasing order

i.e., we can approximate modified Lagrange polynomials on parent clusters by modified Lagrange polynomials in their children. Under moderate conditions, this approximation can be applied repeatedly without harming the total error too much [5, 3], so we can afford to replace the matrices V_{tc} defined in (4) in all non-leaf clusters by approximations.

Definition 4 (Directional cluster basis) *Let $\mathcal{T}_{\mathcal{I}}$ be a cluster tree with a family $\mathcal{D} = (\mathcal{D}_t)_{t \in \mathcal{T}_{\mathcal{I}}}$ of directions. A family $(V_{tc})_{t \in \mathcal{T}_{\mathcal{I}}, c \in \mathcal{D}_t}$ of matrices $V_{tc} \in \mathbb{C}^{\hat{t} \times k}$ is called a directional cluster basis for $\mathcal{T}_{\mathcal{I}}$ and \mathcal{D} if for every $t \in \mathcal{T}_{\mathcal{I}}$ and $t' \in \text{chil}(t)$ there are a direction $c' = \text{dirchil}(t', c)$ and a matrix $E_{t'c} \in \mathbb{C}^{k \times k}$ with*

$$V_{tc}|_{\hat{t} \times k} = V_{t'c'} E_{t'c}. \quad (5)$$

The matrices $E_{t'c}$ are called transfer matrices. Since the matrices V_{tc} have to be stored only for clusters without children, they are called leaf matrices.

Definition 5 (\mathcal{DH}^2 -matrix) *Let $\mathcal{T}_{\mathcal{I}}$ be a cluster tree with a family \mathcal{D} of directions, let $V = (V_{tc})_{t \in \mathcal{T}_{\mathcal{I}}, c \in \mathcal{D}_t}$ be a directional cluster basis, and let $\mathcal{T}_{\mathcal{I} \times \mathcal{I}}$ be a block tree.*

A matrix $G \in \mathbb{C}^{\mathcal{I} \times \mathcal{I}}$ is called a \mathcal{DH}^2 -matrix if for every admissible leaf $b = (t, s) \in \mathcal{L}_{\mathcal{I} \times \mathcal{I}}^+$ there are a direction $c = \text{dirblock}(t, s) \in \mathcal{D}_t \cap \mathcal{D}_s$ and a matrix $S_{ts} \in \mathbb{C}^{k \times k}$ with

$$G|_{\hat{t} \times \hat{s}} = V_{tc} S_{ts} V_{sc}^*. \quad (6)$$

The matrix S_{ts} is called a coupling matrix for the block $b = (t, s)$.

If we have a \mathcal{DH}^2 -matrix, all admissible blocks can be represented by the cluster basis and the coupling matrices. For the inadmissible leaves $b = (t, s) \in \mathcal{L}_{\mathcal{I} \times \mathcal{I}}^-$, we store the corresponding submatrices $G|_{\hat{t} \times \hat{s}}$ explicitly. Under moderate assumptions, these *nearfield matrices* require only $\mathcal{O}(nk)$ units of storage.

For constant wave numbers κ , a \mathcal{DH}^2 -matrix approximation of G requires only $\mathcal{O}(nk^2)$ units of storage. In the high-frequency case, i.e., if $\kappa \sim \sqrt{n}$, a \mathcal{DH}^2 -matrix approximation requires only $\mathcal{O}(nk^2 \log n)$ units of storage [5, 2]. The matrix-vector multiplication can be performed in a similar complexity.

3 Compression of \mathcal{DH}^2 -matrices

Although directional interpolation leads to a robust and fairly fast algorithm for approximating the matrix G , it requires a very large amount of storage, particularly if we are interested in a highly accurate approximation: Figure 1 shows that directional interpolation converges very robustly, but also that interpolation of higher order requires a very large amount of memory, close to 1 TB for the eighth order.

Algebraic compression techniques offer an attractive solution: we use directional interpolation only to provide an intermediate approximation of G and apply algebraic techniques to reduce the rank as far as possible. The resulting re-compression algorithm can be implemented in a way that avoids having to store the entire intermediate \mathcal{DH}^2 -matrix, so that only the final result is written to memory and very large matrices can be handled at high accuracies.

We present here a version of the algorithm introduced in [4] that will be modified in the following sections. Our goal is to find an improved cluster basis $Q = (Q_{tc})_{t \in \mathcal{T}_I, c \in \mathcal{D}_t}$ for the matrix G . In order to avoid redundant information and to ensure numerical stability, we aim for an *isometric* basis, i.e., we require

$$Q_{tc}^* Q_{tc} = I \quad \text{for all } t \in \mathcal{T}_I, c \in \mathcal{D}_t.$$

The best approximation of a matrix block $G|_{\hat{t} \times \hat{s}}$ with respect to this basis is given by the orthogonal projection $Q_{tc} Q_{tc}^* G|_{\hat{t} \times \hat{s}}$, and we have to ensure that all blocks connected to the cluster t and the direction c are approximated. We introduce the sets

$$\mathcal{R}_{tc} := \{s \in \mathcal{T}_I : (t, s) \in \mathcal{T}_{I \times I}, \text{dirblock}(t, s) = c\} \quad \text{for all } t \in \mathcal{T}_I, c \in \mathcal{D}_t \quad (7)$$

containing all column clusters connected to a row cluster t and a given direction c and note that

$$G|_{\hat{t} \times \hat{s}} \approx Q_{tc} Q_{tc}^* G|_{\hat{t} \times \hat{s}} \quad \text{for all } s \in \mathcal{R}_{tc}$$

is a minimal requirement for our new basis. But it is not entirely sufficient: if $t \in \mathcal{T}_I$ has children, Definition 4 requires that $Q_{tc}|_{\hat{t} \times \hat{k}}$ can be expressed in terms of $Q_{t'c'}$ for $t' \in \text{chil}(t)$ and $c' = \text{dirchil}(t', c)$, therefore the basis Q_{tc} has to be able to approximate all admissible blocks connected to the ancestors of t , as well. To reflect this requirement, we extend \mathcal{R}_{tc} to

$$\mathcal{R}_{tc}^* := \begin{cases} \mathcal{R}_{tc} & \text{if } t \text{ is the root of } \mathcal{T}_I, \\ \mathcal{R}_{tc} \cup \bigcup_{\substack{c^+ \in \mathcal{D}_{t^+} \\ \text{dirchil}(t, c^+) = c}} \mathcal{R}_{t^+ c^+}^* & \text{if } t \in \text{chil}(t^+), t^+ \in \mathcal{T}_I \quad \text{for all } t \in \mathcal{T}_I, c \in \mathcal{D}_t \end{cases} \quad (8)$$

by including all admissible blocks connected to the parent, and by induction to any of its ancestors. A suitable cluster basis satisfies

$$G|_{\hat{t} \times \hat{s}} \approx Q_{tc} Q_{tc}^* G|_{\hat{t} \times \hat{s}} \quad \text{for all } s \in \mathcal{R}_{tc}^*, t \in \mathcal{T}_I, c \in \mathcal{D}_t.$$

By combining all of these submatrices in a large matrix

$$G_{tc} := G|_{\hat{t} \times \mathcal{C}_{tc}}, \quad \mathcal{C}_{tc} := \bigcup \{\hat{s} : s \in \mathcal{R}_{tc}^*\},$$

we obtain the equivalent formulation

$$G_{tc} \approx Q_{tc} Q_{tc}^* G_{tc} \quad \text{for all } t \in \mathcal{T}_{\mathcal{I}}, c \in \mathcal{D}_t,$$

and the singular value decompositions of G_{tc} can be used to determine optimal isometric matrices Q_{tc} with this property. The resulting algorithm, investigated in [2], has quadratic complexity, since it does not take the special structure of G into account.

If G is already approximated by a \mathcal{DH}^2 -matrix, e.g., via directional interpolation, we can make this algorithm considerably more efficient. We start by considering the root t of $\mathcal{T}_{\mathcal{I}}$. Let $c \in \mathcal{D}_t$. Since G is a \mathcal{DH}^2 -matrix, we have

$$G|_{\hat{t} \times \hat{s}} = V_{tc} S_{ts} V_{sc}^* \quad \text{for all } s \in \mathcal{R}_{tc},$$

and enumerating $\mathcal{R}_{tc} = \{s_1, \dots, s_m\}$ yields

$$G_{tc} = V_{tc} (S_{ts_1} V_{s_1 c}^* \dots S_{ts_m} V_{s_m c}^*).$$

The right factor has only k rows, and we can use Householder transformations to condense it into a small $k \times k$ matrix without changing the singular values and left singular vectors of G_{tc} . Using the transformations directly, however, is too computationally expensive, so we are looking for way to avoid it.

Definition 6 (Basis weights) *A family $(R_{sc})_{s \in \mathcal{T}_{\mathcal{I}}, c \in \mathcal{D}_s}$ of matrices is called a family of basis weights for the basis $(V_{sc})_{s \in \mathcal{T}_{\mathcal{I}}, c \in \mathcal{D}_s}$ if for every $s \in \mathcal{T}_{\mathcal{I}}$ and $c \in \mathcal{D}_s$ there is an isometric matrix Q_{sc} with*

$$V_{sc} = Q_{sc} R_{sc}$$

and the matrices R_{sc} have each k columns and at most k rows.

If we have basis weights at our disposal, we obtain

$$G_{tc} = V_{tc} (S_{ts_1} R_{s_1 c}^* \dots S_{ts_m} R_{s_m c}^*) \begin{pmatrix} Q_{s_1 c}^* & & \\ & \ddots & \\ & & Q_{s_m c}^* \end{pmatrix},$$

and since the multiplication by an adjoint isometric matrix from the left does not change the singular values or left singular vectors, we can replace G_{tc} with

$$V_{tc} (S_{ts_1} R_{s_1 c}^* \dots S_{ts_m} R_{s_m c}^*).$$

We can even go one step further and compute a thin Householder factorization of the right factor's adjoint

$$\hat{P}_{tc} Z_{tc} = \begin{pmatrix} R_{s_1 c} S_{ts_1}^* \\ \vdots \\ R_{s_m c} S_{ts_m}^* \end{pmatrix}$$

with an isometric matrix \widehat{P}_{tc} and a matrix Z_{tc} that has only k columns and not more than k rows. If we set

$$P_{tc} := \begin{pmatrix} Q_{s_1 c} & & \\ & \ddots & \\ & & Q_{s_m c} \end{pmatrix} \widehat{P}_{tc},$$

we obtain

$$G_{tc} = V_{tc} Z_{tc}^* P_{tc}^*$$

and can drop the rightmost adjoint isometric matrix to work just with the thin matrix $V_{tc} Z_{tc}^*$ that has only at most k columns.

So far, we have only considered the root of the cluster tree. If $t \in \mathcal{T}_{\mathcal{I}}$ is a non-root cluster, it has a parent $t^+ \in \mathcal{T}_{\mathcal{I}}$ and our definition (8) yields

$$\mathcal{R}_{tc}^* = \mathcal{R}_{tc} \cup \bigcup_{\substack{c^+ \in \mathcal{D}_{t^+} \\ \text{dirchil}(t, c^+) = c}} \mathcal{R}_{t^+ c^+}^*.$$

Let $c^+ \in \mathcal{D}_{t^+}$ with $\text{dirchil}(t, c^+) = c$. If we assume that $Z_{t^+ c^+}$ has already been computed, we have

$$G_{tc}|_{\hat{t} \times \mathcal{C}_{t^+ c^+}} = (G_{t^+ c^+})|_{\hat{t} \times \mathcal{C}_{t^+ c^+}} = (V_{t^+ c^+} Z_{t^+ c^+}^* P_{t^+ c^+}^*)|_{\hat{t} \times \mathcal{C}_{t^+ c^+}} = V_{tc} E_{tc^+} Z_{t^+ c^+}^* P_{t^+ c^+}^*.$$

To apply this procedure to all directions c^+ , we enumerate them as

$$\{c_1^+, \dots, c_\ell^+\} = \{c^+ \in \mathcal{D}_{t^+} : \text{dirchil}(t, c^+) = c\}$$

and the admissible blocks again as $\mathcal{R}_{tc} = \{s_1, \dots, s_m\}$ to get

$$\begin{aligned} G_{tc} &= V_{tc} \begin{pmatrix} S_{ts_1} V_{s_1 c}^* & \dots & S_{ts_m} V_{s_m c}^* & E_{tc_1^+} Z_{t^+ c_1^+}^* P_{t^+ c_1^+}^* & \dots & E_{tc_\ell^+} Z_{t^+ c_\ell^+}^* P_{t^+ c_\ell^+}^* \end{pmatrix} \\ &= V_{tc} \begin{pmatrix} S_{ts_1} R_{s_1 c}^* Q_{s_1 c}^* & \dots & S_{ts_m} R_{s_m c}^* Q_{s_m c}^* & E_{tc_1^+} Z_{t^+ c_1^+}^* P_{t^+ c_1^+}^* & \dots & E_{tc_\ell^+} Z_{t^+ c_\ell^+}^* P_{t^+ c_\ell^+}^* \end{pmatrix}. \end{aligned}$$

The rightmost factors are again isometric, and we can once more compute a thin Householder factorization

$$\widehat{P}_{tc} Z_{tc} = \begin{pmatrix} R_{s_1 c} S_{ts_1}^* \\ \vdots \\ R_{s_m c} S_{ts_m}^* \\ Z_{t^+ c_1^+} E_{tc_1^+}^* \\ \vdots \\ Z_{t^+ c_\ell^+} E_{tc_\ell^+}^* \end{pmatrix} \quad \text{and set} \quad P_{tc} := \begin{pmatrix} Q_{s_1 c} & & & & \\ & \ddots & & & \\ & & Q_{s_m c} & & \\ & & & P_{t^+ c_1^+} & \\ & & & & \ddots \\ & & & & & P_{t^+ c_\ell^+} \end{pmatrix} \widehat{P}_{tc}.$$

to obtain

$$G_{tc} = V_{tc} Z_{tc}^* P_{tc}^*$$

Since the isometric matrices P_{tc} do not influence the range of G_{tc} , we do not have to compute them, we only need the weight matrices Z_{tc} .

```

procedure basis_weights( $s$ );
begin
  if  $\text{chil}(s) = \emptyset$  then
    for  $c \in \mathcal{D}_s$  do
      Find a thin Householder decomposition  $V_{sc} = Q_{sc}R_{sc}$ 
  else begin
    for  $s' \in \text{chil}(s)$  do
      basis_weights( $s'$ );
    for  $c \in \mathcal{D}_s$  do begin
      Set up  $\hat{V}_{sc}$  as in (10);
      Find a thin Householder decomposition  $\hat{V}_{sc} = \hat{Q}_{sc}R_{sc}$ 
    end
  end
end

```

Figure 2: Construction of the basis weights R_{sc}

Definition 7 (Total weights) *A family $(Z_{tc})_{t \in \mathcal{T}_I, c \in \mathcal{D}_t}$ of matrices is called a family of total weights for the \mathcal{DH}^2 -matrix G if for every $t \in \mathcal{T}_I$ and $c \in \mathcal{D}_t$ there is an isometric matrix P_{tc} with*

$$G_{tc} = V_{tc}Z_{tc}^*P_{tc}^* \quad (9)$$

and the matrices Z_{tc} have each k columns and at most k rows.

Remark 8 (Symmetric total weights) *In the original approximation constructed by directional interpolation, the same cluster basis is used for rows and columns, since we have $G|_{\hat{t} \times \hat{s}} = V_{tc}S_{ts}V_{sc}^*$ for all admissible blocks $b = (t, s) \in \mathcal{L}_{I \times I}^+$.*

Since the matrix G is not symmetric, this property no longer holds for the adaptively constructed basis $(Q_{tc})_{t \in \mathcal{T}_I, c \in \mathcal{D}_t}$ and we would have to construct a separate basis for the columns by applying the procedure to the adjoint matrix G^ .*

A possible alternative is to extend the total weight matrices to handle G and G^ simultaneously: for every $s \in \mathcal{R}_{tc}$, we include not only $R_{sc}S_{ts}^*$ in the construction of the weight Z_{tc} , but also $R_{sc}S_{st}$. This will give us an adaptive cluster basis that can be used for rows and columns, just like the original. Since the matrices appearing in the Householder factorization are now twice as large, the algorithm will take almost twice as long to complete and the adaptively chosen ranks may increase.*

We can compute the total weights efficiently by this procedure as long as we have the basis weights $(R_{sc})_{s \in \mathcal{T}_I, c \in \mathcal{D}_s}$ at our disposal. These weights can be computed efficiently by taking advantage of their nested structure: if $s \in \mathcal{T}_I$ is a leaf, we compute the thin Householder factorization

$$V_{sc} = Q_{sc}R_{sc}$$

with an isometric matrix Q_{sc} and a matrix R_{sc} with k columns and at most k rows.

If $s \in \mathcal{T}_{\mathcal{I}}$ has children, we first compute the basis weights for all children $\text{chil}(s) = \{s_1, \dots, s_\ell\}$ by recursion and let

$$\widehat{V}_{sc} = \begin{pmatrix} R_{s_1 c_1} E_{s_1 c} \\ \vdots \\ R_{s_\ell c_\ell} E_{s_\ell c} \end{pmatrix}, \quad (10)$$

where $c_i = \text{dirchil}(s_i, c)$ for all $i \in [1 : \ell]$. We compute the thin Householder factorization

$$\widehat{V}_{sc} = \widehat{Q}_{sc} R_{sc}$$

and find

$$V_{sc} = \begin{pmatrix} V_{s_1 c_1} E_{s_1 c} \\ \vdots \\ V_{s_\ell c_\ell} E_{s_\ell c} \end{pmatrix} = \begin{pmatrix} Q_{s_1 c_1} & & \\ & \ddots & \\ & & Q_{s_\ell c_\ell} \end{pmatrix} \widehat{V}_{sc} = \underbrace{\begin{pmatrix} Q_{s_1 c_1} & & \\ & \ddots & \\ & & Q_{s_\ell c_\ell} \end{pmatrix}}_{=:Q_{sc}} \widehat{Q}_{sc} R_{sc}.$$

The matrix Q_{sc} is the product of two isometric matrices and therefore itself isometric. We can see that we can compute the basis weight matrices R_{sc} using only $\mathcal{O}(k^3)$ operations per $s \in \mathcal{T}_{\mathcal{I}}$ and $c \in \mathcal{D}_s$ as long as we are not interested in Q_{sc} . The algorithm is summarized in Figure 2.

Once the basis weights and total weights have been computed, we can construct the improved cluster basis Q_{tc} .

If $t \in \mathcal{T}_{\mathcal{I}}$ is a leaf, we make use of (9) to get

$$G_{tc} = V_{tc} Z_{tc} P_{tc}^*,$$

and we can again drop the isometric matrix P_{tc} and only have to find the singular value decomposition of $V_{tc} Z_{tc}^*$, choose a suitable rank $k_{tc} \in \mathbb{N}_0$ and use the first k_{tc} left singular vectors as columns of the matrix Q_{tc} . We also prepare the matrix $T_{tc} := Q_{tc}^* V_{tc}$ describing the change of basis from V_{tc} to Q_{tc} .

If $t \in \mathcal{T}_{\mathcal{I}}$ is not a leaf, we first construct the basis for all children $\{t_1, \dots, t_\ell\} = \text{chil}(t)$. Since the parent can only approximate what has been kept by its children, we can switch to the orthogonal projection

$$\widehat{G}_{tc} := \begin{pmatrix} Q_{t_1 c_1}^* & & \\ & \ddots & \\ & & Q_{t_\ell c_\ell}^* \end{pmatrix} G_{tc} = \begin{pmatrix} Q_{t_1 c_1}^* G|_{\hat{t}_1 \times \mathcal{C}_{tc}} \\ \vdots \\ Q_{t_\ell c_\ell}^* G|_{\hat{t}_\ell \times \mathcal{C}_{tc}} \end{pmatrix}$$

of G_{tc} with $c_i = \text{dirchil}(t_i, c)$ for all $i \in [1 : \ell]$. Using again (9), we find

$$\widehat{G}_{tc} = \widehat{V}_{tc} Z_{tc} P_{tc}^*,$$

with the projection of V_{tc} into the children's bases

$$\widehat{V}_{tc} := \begin{pmatrix} T_{t_1, c_1} E_{t_1 c} \\ \vdots \\ T_{t_\ell, c_\ell} E_{t_\ell c} \end{pmatrix} \quad (11)$$

```

procedure build_basis( $t$ );
begin
  if  $\text{chil}(t) = \emptyset$  then
    for  $c \in \mathcal{D}_s$  do begin
      Use a thin Householder factorization to get  $Z_{tc}$ ;
      Compute the singular value decomposition  $V_{tc}Z_{tc}^* = U\Sigma V^*$ ;
      Choose a rank  $k_{tc}$ , shrink  $U$  to its first  $k_{tc}$  columns;
       $Q_{tc} \leftarrow U$ ;  $T_{tc} \leftarrow Q_{tc}^*V_{tc}$ 
    end
  else begin
    for  $s' \in \text{chil}(s)$  do
      build_basis( $s'$ );
    for  $c \in \mathcal{D}_s$  do begin
      Use a thin Householder factorization to get  $Z_{tc}$ ;
      Set up  $\widehat{V}_{tc}$  as in (11);
      Compute the singular value decomposition  $\widehat{V}_{tc}Z_{tc}^* = \widehat{U}\Sigma V^*$ ;
      Choose a rank  $k_{tc}$ , shrink  $\widehat{U}$  to its first  $k_{tc}$  columns;
       $\widehat{Q}_{tc} \leftarrow \widehat{U}$ ;  $T_{tc} \leftarrow \widehat{Q}_{tc}^*\widehat{V}_{tc}$ 
    end
  end
end

```

Figure 3: Construction of an adaptive cluster basis

that can be easily computed using the transfer matrices and the basis-change matrices. Once again we can drop the isometric factor P_{tc} and only have to compute the singular value decomposition of $\widehat{V}_{tc}Z_{tc}^*$, choose again a suitable rank $k_{tc} \in \mathbb{N}_0$ and use the first k_{tc} left singular vectors as columns of a matrix \widehat{Q}_{tc} . Using

$$Q_{tc} := \begin{pmatrix} Q_{t_1, c_1} & & \\ & \ddots & \\ & & Q_{t_\ell, c_\ell} \end{pmatrix} \widehat{Q}_{tc}$$

gives us the new cluster basis, where the transfer matrices can be extracted from \widehat{Q}_{tc} . Again it is a good idea to prepare the basis-change matrix $T_{tc} := Q_{tc}^*V_{tc} = \widehat{Q}_{tc}^*\widehat{V}_{tc}$ for the next steps of the recursion.

Under standard assumptions, the entire construction can be performed in $\mathcal{O}(nk^2)$ operations for constant wave numbers and $\mathcal{O}(nk^2 \log n)$ operations in the high-frequency case [4]. The algorithm is summarized in Figure 3. It is important to note that the total weight matrices Z_{tc} can be constructed and discarded during the recursive algorithm, they do not have to be kept in storage permanently. This is in contrast to the basis weight matrices R_{sc} that may appear at any time during the recursion and therefore are kept in storage during the entire run of the algorithm.

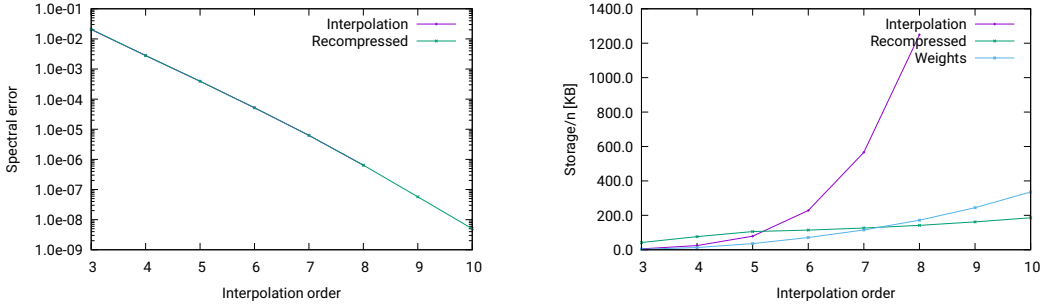


Figure 4: Left: Convergence of recompressed interpolation with increasing order. Right: Storage requirements of original interpolation and recompression

Figure 4 shows that recompression — applied with suitable parameters — leaves the approximation quality unchanged and drastically reduces the storage requirements. The blue curve corresponds to the storage needed for the basis weights, and we can see that it grows beyond the storage for the entire recompressed \mathcal{DH}^2 -matrix if higher polynomial orders are used. This is not acceptable if we want to apply the method to high-frequency problems at high accuracies, so we will now work to reduce the storage requirements for these weights without harming the convergence of the overall method.

4 Error control

In order to preserve the convergence properties, we have to investigate how our algorithm reacts to perturbations.

4.1 Error decomposition

We consider an admissible block $(t, s) \in \mathcal{L}_{\mathcal{I} \times \mathcal{I}}^+$ with $c = \text{dirblock}(t, s)$ that is approximated by our algorithm by

$$Q_{tc}Q_{tc}^*G|_{\hat{t} \times \hat{s}}.$$

If t is a leaf, the approximation error is given by

$$G|_{\hat{t} \times \hat{s}} - Q_{tc}Q_{tc}^*G|_{\hat{t} \times \hat{s}}.$$

If t is not a leaf, there are children $\{t_1, \dots, t_\ell\} = \text{chil}(t)$ with directions $c_i = \text{dirchil}(t_i, c)$, $i \in [1 : \ell]$, and an isometric matrix \hat{Q}_{tc} such that

$$Q_{tc} = \underbrace{\begin{pmatrix} Q_{t_1 c_1} & & \\ & \ddots & \\ & & Q_{t_\ell c_\ell} \end{pmatrix}}_{=:U_{tc}} \hat{Q}_{tc} = U_{tc} \hat{Q}_{tc}$$

and the approximation error can be split into

$$\begin{aligned}
G|_{\hat{t} \times \hat{s}} - Q_{tc} Q_{tc}^* G|_{\hat{t} \times \hat{s}} &= G|_{\hat{t} \times \hat{s}} - U_{tc} \hat{Q}_{tc} \hat{Q}_{tc}^* U_{tc}^* G|_{\hat{t} \times \hat{s}} \\
&= G|_{\hat{t} \times \hat{s}} - U_{tc} U_{tc}^* G|_{\hat{t} \times \hat{s}} + U_{tc} (I - \hat{Q}_{tc} \hat{Q}_{tc}^*) U_{tc}^* G|_{\hat{t} \times \hat{s}} \\
&= \begin{pmatrix} G|_{\hat{t}_1 \times \hat{s}} - Q_{t_1 c_1} Q_{t_1 c_1}^* G|_{\hat{t}_1 \times \hat{s}} \\ \vdots \\ G|_{\hat{t}_\ell \times \hat{s}} - Q_{t_\ell c_\ell} Q_{t_\ell c_\ell}^* G|_{\hat{t}_\ell \times \hat{s}} \end{pmatrix} + U_{tc} (I - \hat{Q}_{tc} \hat{Q}_{tc}^*) U_{tc}^* G|_{\hat{t} \times \hat{s}}.
\end{aligned}$$

The ranges of both terms are perpendicular: for any pair $x, y \in \mathbb{C}^{\hat{s}}$ of vectors we have

$$\begin{aligned}
\langle (G|_{\hat{t} \times \hat{s}} - U_{tc} U_{tc}^* G|_{\hat{t} \times \hat{s}}) x, U_{tc} (I - \hat{Q}_{tc} \hat{Q}_{tc}^*) U_{tc}^* G|_{\hat{t} \times \hat{s}} y \rangle \\
= \langle U_{tc}^* (G|_{\hat{t} \times \hat{s}} - U_{tc} U_{tc}^* G|_{\hat{t} \times \hat{s}}) x, (I - \hat{Q}_{tc} \hat{Q}_{tc}^*) U_{tc}^* G|_{\hat{t} \times \hat{s}} y \rangle \\
= \langle (U_{tc}^* G|_{\hat{t} \times \hat{s}} - U_{tc}^* G|_{\hat{t} \times \hat{s}}) x, (I - \hat{Q}_{tc} \hat{Q}_{tc}^*) U_{tc}^* G|_{\hat{t} \times \hat{s}} y \rangle = 0
\end{aligned}$$

due to $U_{tc}^* U_{tc} = I$. By Pythagoras' theorem, this implies

$$\begin{aligned}
\| (G|_{\hat{t} \times \hat{s}} - Q_{tc} Q_{tc}^* G|_{\hat{t} \times \hat{s}}) x \|^2_2 &= \sum_{i=1}^{\ell} \| (G|_{\hat{t}_i \times \hat{s}} - Q_{t_i c_i} Q_{t_i c_i}^* G|_{\hat{t}_i \times \hat{s}}) x \|^2_2 \\
&\quad + \| (I - \hat{Q}_{tc} \hat{Q}_{tc}^*) U_{tc}^* G|_{\hat{t} \times \hat{s}} x \|^2_2 \quad \text{for all } x \in \mathbb{C}^{\hat{s}},
\end{aligned} \tag{12}$$

i.e., we can split the error *exactly* into contributions of the children and a contribution of the parent t . If the children have children again, we can proceed by induction. To make this precise, we introduce the sets of *descendants*

$$\text{desc}(t, c) := \begin{cases} \{(t, c)\} & \text{if } \text{chil}(t) = \emptyset, \\ \{(t, c)\} \cup \bigcup_{t' \in \text{chil}(t)} \text{desc}(t', \text{dirchil}(t', c)) & \text{otherwise} \end{cases}$$

for all $t \in \mathcal{T}_{\mathcal{I}}$ and $c \in \mathcal{D}_t$.

Theorem 9 (Error representation) *We define*

$$\widehat{G}_{ts} := \begin{cases} G|_{\hat{t} \times \hat{s}} & \text{if } \text{chil}(t) = \emptyset, \\ U_{tc}^* G|_{\hat{t} \times \hat{s}} & \text{otherwise} \end{cases} \quad \text{for all } t, s \in \mathcal{T}_{\mathcal{I}}, c \in \mathcal{D}_t.$$

In the previous section, we have already defined \widehat{Q}_{tc} for non-leaf clusters. We extend this notation by setting $\widehat{Q}_{tc} := Q_{tc}$ for all leaf clusters $t \in \mathcal{T}_{\mathcal{I}}$ and all $c \in \mathcal{D}_t$. Then we have

$$\| (G|_{\hat{t} \times \hat{s}} - Q_{tc} Q_{tc}^* G|_{\hat{t} \times \hat{s}}) x \|^2_2 = \sum_{(t', c') \in \text{desc}(t, c)} \| (\widehat{G}_{t' s} - \widehat{Q}_{t' c'} \widehat{Q}_{t' c'}^* \widehat{G}_{t' s}) x \|^2_2$$

for all $(t, s) \in \mathcal{L}_{\mathcal{I} \times \mathcal{I}}^+$ with $c = \text{dirblock}(t, s)$ and all $x \in \mathbb{C}^{\hat{s}}$.

Proof. With the new notation, (12) takes the form

$$\begin{aligned} \|(G|_{\hat{t} \times \hat{s}} - Q_{tc}Q_{tc}^*G|_{\hat{t} \times \hat{s}})x\|_2^2 &= \sum_{\substack{t' \in \text{chil}(t) \\ c' = \text{dirchil}(t', c)}}^{\ell} \|(G|_{\hat{t}' \times \hat{s}} - Q_{t'c'}Q_{t'c'}^*G|_{\hat{t}' \times \hat{s}})x\|_2^2 \\ &\quad + \|(\hat{G}_{ts} - \hat{Q}_{tc}\hat{Q}_{tc}^*\hat{G}_{ts})x\|_2^2, \end{aligned}$$

and a straightforward induction yields the result. \square

We can see that the matrices \hat{G}_{ts} required by this theorem appear explicitly in the compression algorithm: G_{tc} is the combination of all matrices \hat{G}_{ts} for $s \in \mathcal{R}_{tc}$ if t is a leaf, and otherwise $\hat{G}_{tc} = U_{tc}^*G_{tc} = \hat{V}_{tc}Z_{tc}^*P_{tc}^*$ is the combination of all matrices \hat{G}_{ts} for $s \in \mathcal{R}_{tc}$.

The compression algorithm computes the singular value decompositions of the matrices G_{tc} and \hat{G}_{tc} , respectively, so we have all the singular values at our disposal to guarantee $\|G_{tc} - Q_{tc}Q_{tc}^*G_{tc}\|_2 \leq \epsilon$ or $\|\hat{G}_{tc} - \hat{Q}_{tc}\hat{Q}_{tc}^*\hat{G}_{tc}\|_2 \leq \epsilon$, respectively, for any given accuracy $\epsilon \in \mathbb{R}_{>0}$ by ensuring that the first dropped singular value $\sigma_{k_{tc}+1}$ is less than ϵ .

4.2 Block-relative error control

Although multiple submatrices are combined in G_{tc} , they do not all have to be treated identically [1, Chapter 6.8]: we can scale the different submatrices with individually chosen weights, e.g., given $t \in \mathcal{T}_{\mathcal{I}}$ and $c \in \mathcal{D}_t$, we can choose a weight $\omega_{ts} \in \mathbb{R}_{>0}$ for every $s \in \mathcal{R}_{tc}^*$ and replace G_{tc} by

$$G_{\omega,tc} := (\omega_{ts_1}^{-1}G|_{\hat{t} \times \hat{s}_1} \quad \dots \quad \omega_{ts_m}^{-1}G|_{\hat{t} \times \hat{s}_m})$$

with the enumeration $\mathcal{R}_{tc}^* = \{s_1, \dots, s_m\}$. Correspondingly, \hat{G}_{tc} is replaced by a weighted version $\hat{G}_{\omega,tc}$ and Z_{tc} by $Z_{\omega,tc}$. The modified algorithm will now guarantee

$$\begin{aligned} \|\hat{G}_{ts} - \hat{Q}_{tc}\hat{Q}_{tc}^*\hat{G}_{ts}\|_2 &= \omega_{ts}\|G_{\omega,tc}|_{\hat{t} \times \hat{s}} - Q_{tc}Q_{tc}^*G_{\omega,tc}|_{\hat{t} \times \hat{s}}\|_2 \\ &\leq \omega_{ts}\|G_{\omega,tc} - Q_{tc}Q_{tc}^*G_{\omega,tc}\|_2 \leq \omega_{ts}\epsilon \end{aligned}$$

for leaf clusters $t \in \mathcal{T}_{\mathcal{I}}$ and

$$\begin{aligned} \|\hat{G}_{ts} - \hat{Q}_{tc}\hat{Q}_{tc}^*\hat{G}_{ts}\|_2 &= \omega_{ts}\|U_t^*G_{\omega,tc}|_{\hat{t} \times \hat{s}} - \hat{Q}_{tc}\hat{Q}_{tc}^*U_t^*G_{\omega,tc}|_{\hat{t} \times \hat{s}}\|_2 \\ &\leq \omega_{ts}\|\hat{G}_{\omega,tc} - \hat{Q}_{tc}\hat{Q}_{tc}^*\hat{G}_{\omega,tc}\|_2 \leq \omega_{ts}\epsilon \end{aligned}$$

for non-leaf clusters. With these modifications, Theorem 9 yields

$$\|(G|_{\hat{t} \times \hat{s}} - Q_{tc}Q_{tc}^*G|_{\hat{t} \times \hat{s}})x\|_2^2 \leq \sum_{(t',c') \in \text{desc}(t,c)} \omega_{t's}^2 \epsilon^2 \quad \text{for all } (t,s) \in \mathcal{L}_{\mathcal{I} \times \mathcal{I}}^+. \quad (13)$$

The weights ω_{ts} can be used to keep the error closely under control. As an example, we consider how to implement *block-relative* error controls, i.e., how to ensure

$$\|G|_{\hat{t} \times \hat{s}} - Q_{tc}Q_{tc}^*G|_{\hat{t} \times \hat{s}}\|_2 \leq \epsilon\|G|_{\hat{t} \times \hat{s}}\|$$

for a block $(t, s) \in \mathcal{L}_{\mathcal{I} \times \mathcal{I}}^+$. We start by observing that we have

$$\|G|_{\hat{t} \times \hat{s}}\|_2 = \|V_{tc}S_{ts}V_{sc}^*\|_2 = \|R_{tc}S_{ts}R_{sc}^*\|_2$$

due to the admissibility and using the basis weights introduced in Definition 6, so the spectral norm can be computed efficiently.

We assume that a cluster can have at most m children and set

$$\omega_{t's} := \begin{cases} \frac{1}{\sqrt{m+1}} \|G|_{\hat{t} \times \hat{s}}\|_2 & \text{if } t' = t, \\ \frac{1}{\sqrt{m+1}} \omega_{t+s} & \text{if } t' \in \text{chil}(t^+) \end{cases} \quad \text{for all } (t', c') \in \text{desc}(t, c).$$

Keeping in mind that every cluster can have at most m children, substituting $\omega_{t's}$ in (13) and summing up level by level yields

$$\|G|_{\hat{t} \times \hat{s}} - Q_{tc}Q_{tc}^*G|_{\hat{t} \times \hat{s}}\|_2^2 \leq \sum_{(t', c') \in \text{desc}(t, c)} \omega_{t's}^2 \epsilon^2 \leq \sum_{\ell=0}^{\infty} \left(\frac{m}{m+1} \right)^\ell \omega_{ts}^2 \epsilon^2,$$

allowing us to evaluate the geometric sum to conclude

$$\|G|_{\hat{t} \times \hat{s}} - Q_{tc}Q_{tc}^*G|_{\hat{t} \times \hat{s}}\|_2^2 \leq \frac{1}{1 - \frac{m}{m+1}} \omega_{ts}^2 \epsilon^2 = (m+1) \omega_{ts}^2 \epsilon^2 = \epsilon^2 \|G|_{\hat{t} \times \hat{s}}\|_2^2.$$

The weights $\omega_{t's}$ can be computed and conveniently included during the construction of the total weights at only minimal additional cost.

4.3 Stability

In order to improve the efficiency of our algorithm, we would like to replace the \mathcal{DH}^2 -matrix G by an approximation. If we want to ensure that the result of the compression algorithm is still useful, we have to investigate its stability. In the following, G denotes the matrix treated during the compression algorithm, while H denotes the matrix that we actually want to approximate.

Lemma 10 (Stability) *Let $H \in \mathbb{C}^{\mathcal{I} \times \mathcal{I}}$. We have*

$$\|(H|_{\hat{t} \times \hat{s}} - Q_{tc}Q_{tc}^*H|_{\hat{t} \times \hat{s}})x\|_2 \leq \|(G|_{\hat{t} \times \hat{s}} - Q_{tc}Q_{tc}^*G|_{\hat{t} \times \hat{s}})x\|_2 + \|(H|_{\hat{t} \times \hat{s}} - G|_{\hat{t} \times \hat{s}})x\|_2$$

for all $(t, s) \in \mathcal{L}_{\mathcal{I} \times \mathcal{I}}^+$ with $c = \text{dirblock}(t, s)$ and all $x \in \mathbb{C}^{\hat{s}}$.

Proof. Let $(t, s) \in \mathcal{L}_{\mathcal{I} \times \mathcal{I}}^+$, $c = \text{dirblock}(t, s)$ and $x \in \mathbb{C}^{\hat{s}}$. We have

$$\begin{aligned} H|_{\hat{t} \times \hat{s}} - Q_{tc}Q_{tc}^*H|_{\hat{t} \times \hat{s}} &= G|_{\hat{t} \times \hat{s}} + (H - G)|_{\hat{t} \times \hat{s}} - Q_{tc}Q_{tc}^*G|_{\hat{t} \times \hat{s}} - Q_{tc}Q_{tc}^*(H - G)|_{\hat{t} \times \hat{s}} \\ &= G|_{\hat{t} \times \hat{s}} - Q_{tc}Q_{tc}^*G|_{\hat{t} \times \hat{s}} + (I - Q_{tc}Q_{tc}^*)(H - G)|_{\hat{t} \times \hat{s}} \end{aligned}$$

and therefore by the triangle inequality

$$\|(H|_{\hat{t} \times \hat{s}} - Q_{tc}Q_{tc}^*H|_{\hat{t} \times \hat{s}})x\|_2 \leq \|(G|_{\hat{t} \times \hat{s}} - Q_{tc}Q_{tc}^*G|_{\hat{t} \times \hat{s}})x\|_2 + \|(I - Q_{tc}Q_{tc}^*)(H - G)x\|_2.$$

We let $y := (H - G)|_{\hat{t} \times \hat{s}} x$ and make use of the isometry of Q_{tc} to find

$$\begin{aligned} \|(I - Q_{tc}Q_{tc}^*)y\|_2^2 &= \|y\|_2^2 - \langle y, Q_{tc}Q_{tc}^*y \rangle_2 - \langle Q_{tc}Q_{tc}^*y, y \rangle_2 + \|Q_{tc}Q_{tc}^*y\|_2^2 \\ &= \|y\|_2^2 - 2\langle y, Q_{tc}Q_{tc}^*Q_{tc}Q_{tc}^*y \rangle_2 + \|Q_{tc}Q_{tc}^*y\|_2^2 \\ &= \|y\|_2^2 - 2\langle Q_{tc}Q_{tc}^*y, Q_{tc}Q_{tc}^*y \rangle_2 + \|Q_{tc}Q_{tc}^*y\|_2^2 \\ &= \|y\|_2^2 - \|Q_{tc}Q_{tc}^*y\|_2^2 \leq \|y\|_2^2. \end{aligned}$$

Since this is equivalent with $\|(I - Q_{tc}Q_{tc}^*)(H - G)|_{\hat{t} \times \hat{s}} x\|_2^2 \leq \|(H - G)|_{\hat{t} \times \hat{s}} x\|_2^2$, the proof is complete. \square

This lemma implies that if we want to approximate a matrix H , but apply the algorithm to an approximation G satisfying the block-relative error estimate

$$\|H|_{\hat{t} \times \hat{s}} - G|_{\hat{t} \times \hat{s}}\|_2 \leq \epsilon\|H|_{\hat{t} \times \hat{s}}\|_2 \quad \text{for all } (t, s) \in \mathcal{L}_{\mathcal{I} \times \mathcal{I}}^+,$$

we will obtain

$$\begin{aligned} \|H|_{\hat{t} \times \hat{s}} - Q_{tc}Q_{tc}^*H|_{\hat{t} \times \hat{s}}\|_2 &\leq \|G|_{\hat{t} \times \hat{s}} - Q_{tc}Q_{tc}^*G|_{\hat{t} \times \hat{s}}\|_2 + \|H|_{\hat{t} \times \hat{s}} - G|_{\hat{t} \times \hat{s}}\|_2 \\ &\leq \epsilon\|G|_{\hat{t} \times \hat{s}}\|_2 + \epsilon\|H|_{\hat{t} \times \hat{s}}\|_2 \\ &\leq \epsilon(\|H|_{\hat{t} \times \hat{s}}\|_2 + \|G - H|_{\hat{t} \times \hat{s}}\|_2) + \epsilon\|H|_{\hat{t} \times \hat{s}}\|_2 \\ &\leq \epsilon(1 + \epsilon)\|H|_{\hat{t} \times \hat{s}}\|_2 + \epsilon\|H|_{\hat{t} \times \hat{s}}\|_2 \\ &= \epsilon(2 + \epsilon)\|H|_{\hat{t} \times \hat{s}}\|_2, \end{aligned}$$

i.e., the basis constructed to ensure block-relative error estimates for the matrix G will also ensure block-relative error estimates for the matrix H , only with a slightly larger error factor $\approx 2\epsilon$. Since our error-control strategy can ensure any accuracy $\epsilon > 0$, this is quite satisfactory.

5 Approximated weights

Figure 4 suggests that for higher accuracies, the basis weights $(R_{sc})_{s \in \mathcal{T}_{\mathcal{I}}, c \in \mathcal{D}_s}$ can require more storage than the entire recompressed \mathcal{DH}^2 -matrix. With the error representation of Theorem 9 and the stability analysis of the previous section at our disposal, we can investigate ways to reduce the storage requirements without causing significant harm to the final result.

We do not have to worry about the total weights $(Z_{tc})_{t \in \mathcal{T}_{\mathcal{I}}, c \in \mathcal{D}_t}$, since they can be set up during the recursive construction of the adaptive cluster basis.

5.1 Direct approximation of weights.

The basis weight matrices R_{sc} are required by our algorithm when it sets up the total weight matrix Z_{tc} with

$$G_{tc} = V_{tc}Z_{tc}^*P_{tc}^*$$

using

$$G_{tc}|_{\hat{t} \times \hat{s}} = V_{tc} S_{ts} W_{sc}^* = V_{tc} S_{ts} R_{sc}^* Q_{sc}^*$$

for an admissible block $b = (t, s) \in \mathcal{L}_{\mathcal{I} \times \mathcal{I}}^+$. The isometric matrix Q_{sc} influences only P_{tc} and can be dropped since it does not influence the singular values or the left singular vectors.

Our goal is to replace the basis weight R_{sc} by an approximation \tilde{R}_{sc} while ensuring that the recompression algorithm keeps working reliably. We find

$$\|G_{tc}|_{\hat{t} \times \hat{s}} - V_{tc} S_{ts} \tilde{R}_{sc}^* Q_{sc}^*\|_2 = \|V_{tc} S_{ts} (R_{sc}^* - \tilde{R}_{sc}^*) Q_{sc}^*\|_2 = \|V_{tc} S_{ts} (R_{sc} - \tilde{R}_{sc})^*\|_2$$

and conclude that it is sufficient to ensure that the product $\tilde{R}_{sc} S_{ts}^*$ is a good approximation of the product $R_{sc} S_{ts}^*$, we do not require \tilde{R}_{sc} itself to be a good approximation of R_{sc} . This is a crucial observation, because important approximation properties are due to the kernel function represented by S_{ts} , not due to the essentially arbitrary polynomial basis represented by R_{sc} .

Since the basis weight R_{sc} will be used for multiple clusters $t \in \mathcal{T}_{\mathcal{I}}$, we introduce the sets

$$\mathcal{C}_{sc} := \{t \in \mathcal{T}_{\mathcal{I}} : (t, s) \in \mathcal{T}_{\mathcal{I} \times \mathcal{I}}, \text{dirblock}(t, s) = c\} \quad \text{for all } s \in \mathcal{T}_{\mathcal{I}}, c \in \mathcal{D}_s \quad (14)$$

in analogy to the sets \mathcal{R}_{tc} used for the compression algorithm in (7). Enumerating the elements by $\mathcal{C}_{sc} = \{t_1, \dots, t_m\}$ leads us to consider the approximation of the matrix

$$W_{sc} := R_{sc} (S_{t_1 s}^* \ \dots \ S_{t_m s}^*). \quad (15)$$

The optimal solution is again provided by the singular value decomposition of W_{sc} : for the singular values $\sigma_1, \sigma_2, \dots$ and a given accuracy $\epsilon \in \mathbb{R}_{>0}$, we choose a rank $k_{sc} \in \mathbb{N}$ such that $\sigma_{k_{sc}+1} \leq \epsilon$ and combine the first k_{sc} left singular vectors in an isometric matrix Q_{sc} . We define $\tilde{R}_{sc} := Q_{sc}^* R_{sc}$ and find

$$\|R_{sc} S_{st}^* - Q_{sc} \tilde{R}_{sc} S_{st}^*\|_2 = \|R_{sc} S_{st}^* - Q_{sc} Q_{sc}^* R_{sc} S_{st}^*\|_2 \leq \|W_{sc} - Q_{sc} Q_{sc}^* W_{sc}\|_2 \leq \epsilon.$$

The resulting algorithm is summarized in Figure 5. It is important to note that the original basis weights R_{sc} are discarded as soon as they are no longer needed so that the original weights have to be kept in storage only for the children of the current cluster and the children of its ancestors at every point of the algorithm.

5.2 Block-relative error control

Again, we are interested in blockwise relative error estimates, and as before, we can modify the blockwise approximation by introducing weights $\omega_{ts} \in \mathbb{R}_{>0}$ and considering

$$W_{\omega, sc} := R_{sc} (\omega_{t_1 s}^{-1} S_{t_1 s}^* \ \dots \ \omega_{t_m s}^{-1} S_{t_m s}^*). \quad (16)$$

Replacing W_{sc} by $W_{\omega, sc}$ yields

$$\begin{aligned} \|R_{sc} S_{st}^* - \tilde{R}_{sc} S_{st}^*\|_2 &= \omega_{ts} \|R_{sc} \omega_{ts}^{-1} S_{st}^* - Q_{sc} Q_{sc}^* R_{sc} \omega_{ts}^{-1} S_{st}^*\|_2 \\ &\leq \omega_{ts} \|W_{\omega, sc} - Q_{sc} Q_{sc}^* W_{\omega, sc}\|_2 \leq \omega_{ts} \epsilon. \end{aligned}$$

```

procedure approx_weights( $s$ );
begin
  if  $\text{chil}(s) = \emptyset$  then
    for  $c \in \mathcal{D}_s$  do begin
      Find a thin Householder decomposition  $V_{sc} = Q_{sc}R_{sc}$ ;
      Set up  $W_{sc}$  as in (15) or (16);
      Compute the singular value decomposition  $W_{sc} = U\Sigma V^*$ ;
      Choose a rank  $k_{sc}$ , shrink  $U$  to its first  $k_{sc}$  columns;
       $\tilde{R}_{sc} \leftarrow U^*R_{sc}$ 
    end
  else begin
    for  $s' \in \text{chil}(s)$  do
      approx_weights( $s'$ );
    for  $c \in \mathcal{D}_s$  do begin
      Set up  $\hat{V}_{sc} \in \mathbb{C}^{M_{sc} \times k}$  as in (10);
      Find a thin Householder decomposition  $\hat{V}_{sc} = \hat{Q}_{sc}\hat{R}_{sc}$ ;
      Set up  $W_{sc}$  as in (15) or (16);
      Compute the singular value decomposition  $W_{sc} = U\Sigma V^*$ ;
      Choose a rank  $k_{sc}$ , shrink  $U$  to its first  $k_{sc}$  columns;
       $\tilde{R}_{sc} \leftarrow U^*R_{sc}$ 
    end;
    for  $s' \in \text{chil}(s)$ ,  $c' \in \mathcal{D}_{s'}$  do
      Discard  $R_{s'c'}$  from memory
    end
  end

```

Figure 5: Construction of the basis weights R_{sc}

For the blockwise error we obtain

$$\begin{aligned}
\|G|_{\hat{t} \times \hat{s}} - V_{tc}S_{ts}\tilde{R}_{sc}^*Q_{sc}^*\|_2 &= \|V_{tc}S_{ts}(R_{sc} - \tilde{R}_{sc})^*\|_2 \\
&\leq \|V_{tc}\|_2\|(R_{sc} - \tilde{R}_{sc})S_{ts}^*\|_2 \leq \|V_{tc}\|_2\omega_{ts}\epsilon,
\end{aligned}$$

so a relative error bound is guaranteed if we ensure

$$\omega_{ts} \leq \frac{\|V_{tc}S_{ts}V_{sc}^*\|_2}{\|V_{tc}\|_2}.$$

Evaluating the numerator and denominator exactly would require us again to have the full basis weights at our disposal. Fortunately, a projection is sufficient for our purposes: in a preparation step, we compute the basis weight R_{tc} , find its singular value decomposition and use a given number $k_{\text{norm}} \in \mathbb{N}$ of left singular vectors to form an auxiliary isometric matrix P_{tc} and store $N_{tc} := P_{tc}^*R_{rc}$. Since the first singular value corresponds

to the spectral norm of R_{tc} , and therefore the spectral norm of V_{tc} , we have

$$\|N_{tc}\|_2 = \|P_{tc}^* R_{tc}\|_2 = \|R_{tc}\|_2 = \|V_{tc}\|_2$$

and can evaluate the denominator exactly. Since $P_{tc}P_{tc}^*$ is an orthogonal projection, we also have

$$\|V_{tc}S_{ts}V_{sc}^*\|_2 = \|R_{tc}S_{ts}R_{sc}^*\|_2 \geq \|P_{tc}^* R_{tc}S_{ts}R_{sc}^* P_{sc}\|_2 = \|N_{tc}S_{ts}N_{sc}^*\|_2,$$

i.e., we can find a lower bound for the numerator. Fortunately, a lower bound is sufficient for our purposes, and we can use

$$\omega_{ts} := \frac{\|N_{tc}S_{ts}N_{sc}^*\|_2}{\|N_{tc}\|_2} \leq \frac{\|V_{tc}S_{ts}V_{sc}^*\|_2}{\|V_{tc}\|_2}.$$

The algorithm for constructing the norm-estimation matrices N_{tc} is summarized in Figure 6. It uses exact Householder factorizations $Q_{tc}R_{rc} = V_{tc}$ for all basis matrices and then truncates R_{tc} . In order to make the computation efficient, we use

$$V_{tc} = \begin{pmatrix} V_{t_1,c_1} E_{t_1c} \\ \vdots \\ V_{t_n,c_n} E_{t_nc} \end{pmatrix} = \begin{pmatrix} Q_{t_1,c_1} & & \\ & \ddots & \\ & & Q_{t_n,c_n} \end{pmatrix} \widehat{V}_{tc}, \quad \widehat{V}_{tc} := \begin{pmatrix} R_{t_1,c_1} E_{t_1c} \\ \vdots \\ R_{t_n,c_n} E_{t_nc} \end{pmatrix} \quad (17)$$

to replace V_{tc} by the projected matrix \widehat{V}_{tc} with $\text{chil}(t) = \{t_1, \dots, t_n\}$ and $c_i = \text{dirchil}(t_i, c)$ for all $i \in [1 : n]$.

Figure 7 shows that compressing the basis weights following these principles leaves the accuracy of the matrix intact and significantly reduces the storage requirements.

6 Numerical experiments

To demonstrate the properties of the new algorithms in practical applications, we consider direct boundary integral formulations for the Helmholtz problem on the unit sphere. We create a mesh for the unit sphere by starting with a double pyramid $P = \{x \in \mathbb{R}^3 : |x_1| + |x_2| + |x_3| = 1\}$ and refining each of its faces into m^2 triangles, where $m \in \{16, 24, 32, 48, \dots, 1024\}$. Projecting these triangles' vertices to the unit sphere yields regular surface meshes with between 2 048 and 8 388 608 triangles.

We discretize the direct boundary integral formulations for the Dirichlet-to-Neumann and the Neumann-to-Dirichlet problem with piecewise constant basis functions for the Neumann values and continuous linear nodal basis functions for the Dirichlet values. The approximation of the single-layer matrix by a \mathcal{DH}^2 -matrix has already been discussed.

For the double-layer matrix, we apply directional interpolation to the kernel function and take the normal derivative of the result. This again yields an \mathcal{DH}^2 -matrix. The approximation error has been investigated in [3].

For the hypersingular matrix, we use partial integration [9, Corollary 3.3.24] and again apply directional interpolation to the remaining kernel function.

```

procedure approx_norms( $t$ );
begin
  if  $\text{chil}(t) = \emptyset$  then
    for  $c \in \mathcal{D}_t$  do begin
      Find a thin Householder decomposition  $V_{tc} = Q_{tc}R_{tc}$ ;
      Compute the singular value decomposition  $R_{tc} = U\Sigma V^*$ ;
      Shrink  $U$  to its first  $k_{\text{norm}}$  columns;
       $N_{tc} \leftarrow U^*R_{tc}$ 
    end
  else begin
    for  $t' \in \text{chil}(t)$  do
      approx_norms( $t'$ );
    for  $c \in \mathcal{D}_t$  do begin
      Set up  $\hat{V}_{tc}$  as in (17);
      Find a thin Householder decomposition  $\hat{V}_{tc} = \hat{Q}_{tc}R_{tc}$ 
      Compute the singular value decomposition  $R_{tc} = U\Sigma V^*$ ;
      Shrink  $U$  to its first  $k_{\text{norm}}$  columns;
       $N_{tc} \leftarrow U^*R_{tc}$ 
    end;
    for  $t' \in \text{chil}(t)$ ,  $c' \in \mathcal{D}_{t'}$  do
      Discard  $R_{t'c'}$  from memory
  end
end

```

Figure 6: Construction of norm-approximation matrices N_{tc}

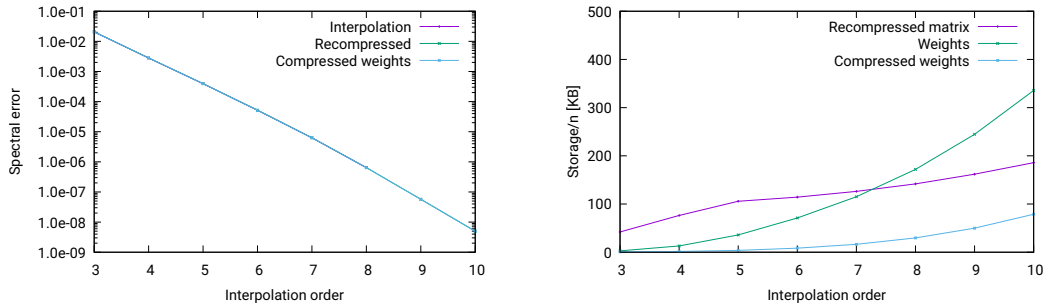


Figure 7: Left: Convergence of recompressed interpolation with compressed weights.
Right: Storage requirements of compressed and uncompressed weights

n	m	Weight φ_i			SLP			DLP		
		Norm	Comp	Mem	Row	Col	Mem	Row	Col	Mem
8 192	3	< 0.1	1.6	3	0.8	0.8	319	0.3	0.3	331
18 432	4	0.1	3.0	20	1.8	1.5	588	1.2	1.3	648
32 768	4	0.1	9.1	41	2.7	2.7	943	2.3	2.5	951
73 728	5	0.4	38.8	195	4.2	4.3	2013	3.3	3.7	1792
131 072	5	1.2	57.7	403	7.4	7.9	3594	6.1	7.0	3243
294 912	5	2.7	104.8	1024	16.8	17.4	8234	11.9	13.2	7774
524 288	6	9.1	272.5	3293	55.1	52.7	15797	43.7	35.7	13959
1 179 648	6	19.0	488.9	8234	126.6	120.5	37949	95.9	82.6	35281
2 097 152	7	46.8	1877.9	23702	806.7	828.6	71768	624.5	517.2	62031
4 718 592	7	125.9	3922.9	59791	2290.7	1786.9	176761	1480.1	1235.6	162386
8 388 608	7	235.3	6924.8	115097	3536.6	3218.0	332950	2613.9	2369.1	323817

Table 1: Helmholtz boundary integral equation with constant wave number $\kappa = 4$

In order to save storage, basis weights for the row and column basis of the single-layer matrix and the row basis of the double-layer matrix are shared, and basis weights for the column basis of the double-layer matrix and the row and column basis of the hypersingular matrix are also shared. In our implementation, this can be easily accomplished by including more matrix blocks in the matrices W_{sc} .

The resulting systems of linear equations are solved by a GMRES method that is preconditioned using an \mathcal{H} -LU factorization [7, Chapter 7.6] of a coarse approximation of the $\mathcal{D}\mathcal{H}^2$ -matrix.

Table 1 contains results for a first experiment with the constant wave number $\kappa = 4$. The column “n” gives the number of triangles, the column “m” gives the order of the interpolation, the column “Norm” gives the time in seconds for the approximation of the matrix norm with the algorithm given in Figure 6, the column “Comp” gives the time for the compression of the weights by the algorithm in Figure 5 and “Mem” the storage requirements in MB.

The columns “Row” and “Col” give the times in seconds for constructing the adaptive row and column cluster bases, both for the single-layer and the double-layer matrix, while the columns “Mem” give the storage requirements in MB for the compressed $\mathcal{D}\mathcal{H}^2$ -matrices.

The experiment was performed on a server with two AMD EPYC 7713 processors with 64 cores each and a total of 2 048 GB of memory.

We can see that the runtimes and storage requirements grow slowly with increasing matrix dimension and increasing polynomial order, as predicted by the theory. Truncation tolerances were chosen to ensure that the convergence of the original Galerkin discretization is preserved, i.e., we obtain L^2 -norm errors falling like $\mathcal{O}(h)$ for the Dirichlet-to-Neumann problem and like $\mathcal{O}(h^2)$ for the Neumann-to-Dirichlet problem.

Table 2 contains results for a second experiment with the a wave number that grows

n	κ	m	Weight φ_i			Row	SLP Col	Mem	DLP		
			Norm	Comp	Mem				Row	Col	Mem
8 192	4	3	< 0.1	1.6	3	0.7	0.8	319	0.3	0.6	331
18 432	6	4	0.1	4.4	20	2.7	3.1	993	1.5	1.6	1057
32 768	8	4	0.1	38.3	43	6.5	7.2	2295	4.1	3.6	2336
73 728	12	5	0.4	128.8	228	18.7	19.3	7318	15.7	15.6	7507
131 072	16	5	1.3	303.2	517	39.9	40.6	16888	36.6	33.8	17170
294 912	24	5	4.5	817.6	1781	110.4	109.0	43792	94.0	93.8	45345
524 288	32	6	20.9	3118.1	6666	362.4	337.1	94766	353.1	364.1	93371
1 179 648	48	6	88.4	10039.7	20607	968.5	1009.5	255373	1223.4	1072.9	259687
2 097 152	64	7	277.2	46939.6	74749	6005.4	6067.7	455584	5838.1	5036.8	438976

Table 2: Helmholtz boundary integral equation with growing wave number

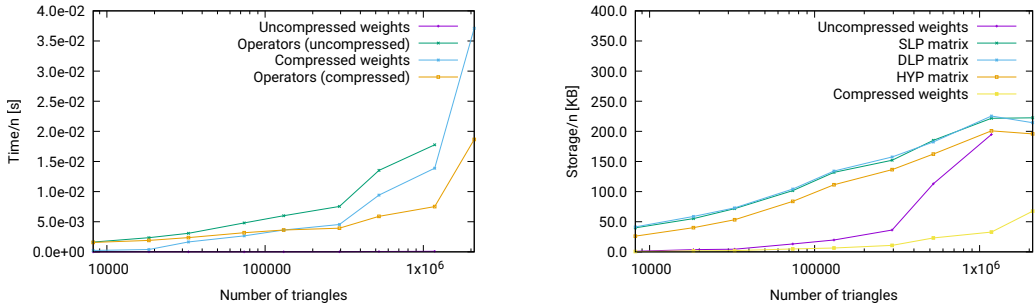


Figure 8: Left: Runtime per degree of freedom. Right: Storage requirements per degree of freedom

as the mesh is refined. This is common in practical applications when the mesh is chosen just fine enough to resolve waves.

The growing wave number makes it significantly harder to satisfy the admissibility condition (3a) and thereby leads to an increase in blocks that have to be treated. The admissibility condition (3b) implies that we also have to introduce a growing number of directions as the wave number increases.

The results of our experiment show the expected increase both in computing time and storage requirements: for 2 097 152 triangles, the setup takes five to six times as long as in the low-frequency case, and both the weight matrices and the final compressed $\mathcal{D}\mathcal{H}^2$ -matrices require far more storage.

For very large meshes with a high interpolation order, setting up the compressed weight matrices takes far longer than the subsequent construction of the $\mathcal{D}\mathcal{H}^2$ -matrices. This can be attributed to the fact that the algorithm in Figure 5 has to compute singular value decompositions of the original coupling matrices, and these matrices have $\mathcal{O}(m^6)$

coefficients. A possible solution may be to replace the coupling matrices by low-rank approximations. Our results in Section 4 indicate that this will not harm the overall algorithm as long as the approximations satisfy block-relative error bounds.

Figure 8 illustrates the algorithms' practical performance: the left figure shows the runtime per degree of freedom using a logarithmic scale for the number of triangles. We can see that the runtimes grow like $\mathcal{O}(n \log n)$, as predicted, with the slope depending on the order of interpolation.

The right figure shows the storage, again per degree of freedom, and we can see that the compressed $\mathcal{D}\mathcal{H}^2$ -matrices for the three operators show the expected $\mathcal{O}(n \log n)$ behaviour. The compressed weights grow slowly, while the uncompressed weights appear to be set to surpass the storage requirements of the matrices they are used to construct.

References

- [1] S. Börm. *Efficient Numerical Methods for Non-local Operators: \mathcal{H}^2 -Matrix Compression, Algorithms and Analysis*, volume 14 of *EMS Tracts in Mathematics*. EMS, 2010.
- [2] S. Börm. Directional \mathcal{H}^2 -matrix compression for high-frequency problems. *Num. Lin. Alg. Appl.*, 24(6):e2112, 2017.
- [3] S. Börm. On iterated interpolation. *SIAM Num. Anal.*, 60(6):3124–3144, 2022.
- [4] S. Börm and C. Börst. Hybrid matrix compression for high-frequency problems. *SIAM Matrix Anal. Appl.*, 41((4)):1704–1725, 2020.
- [5] S. Börm and J. M. Melenk. Approximation of the high-frequency Helmholtz kernel by nested directional interpolation: error analysis. *Numer. Math.*, 137(1):1–34, 2017.
- [6] A. Brandt. Multilevel computations of integral transforms and particle interactions with oscillatory kernels. *Comp. Phys. Comm.*, 65(1–3):24–38, 1991.
- [7] W. Hackbusch. *Hierarchical Matrices: Algorithms and Analysis*. Springer, 2015.
- [8] M. Messner, M. Schanz, and E. Darve. Fast directional multilevel summation for oscillatory kernels based on Chebyshev interpolation. *J. Comp. Phys.*, 231(4):1175–1196, 2012.
- [9] S. A. Sauter and C. Schwab. *Boundary Element Methods*. Springer, 2011.